Article

A Systematical Rheological Study of Maize Kernel

Shaoyang Sheng [1], Aimin Shi [2],* and Junjie Xing [3]

1   School of Public Health, Anhui Medical University, Hefei 230032, China
2   Institute of Food Science and Technology, Chinese Academy of Agricultural Sciences, Key Laboratory of
    Agro-Products Processing, Ministry of Agriculture and Rural Affairs, Beijing 100193, China
3   State Key Laboratory of Food Science and Technology, School of Food Science and Technology,
    Jiangnan University, Wuxi 214122, China
*   Correspondence: shiaimin@caas.cn

Abstract: In this study, the rheological behavior of maize kernel was systematically investigated using a dynamic mechanical analyzer. The loss in toughness caused by drying resulted in a downward shift in the relaxation curve and an upward shift in the creep curve. The long relaxation behavior became obvious when the temperature was above 45 °C, resulting from the weakening of hydrogen bonds with temperature. The maize kernel relaxed more rapidly at high temperatures, caused by a reduction in the cell wall viscosity and polysaccharide tangles. The Deborah numbers were all much smaller than one, suggesting that the Maxwell elements showed viscous behavior. Maize kernel, as a viscoelastic material, showed a dominant viscous property at high temperatures. The decline in β with increasing drying temperature indicated an increase in the width of the relaxation spectrum. A Hookean spring elastic portion made up the majority of the maize kernel creep strain. The order–disorder transformation zone of maize kernel was about 50–60 °C. Due to the complexity of maize kernel, the William–Landel–Ferry constants differed from the universal values; these constants should be ascertained through experiments. Time-temperature superposition was successfully used to describe the rheological behavior. The results show that maize kernel is a thermorheologically simple material. The data acquired in this study can be used for maize processing and storage.

Keywords: rheological properties; time-temperature superposition principle; maize kernel

1. Introduction

As an important staple crop, maize is widely grown throughout the world [1]. The water content of maize at harvest ranges from 20% to 28% [2]. For safe storage, maize should be dried to a 12–13% water content [3].

Maize can be dried by many methods, such as hot air drying, vacuum drying, solar drying, and microwave drying. Hot air drying is a procedure in which a product is dried with heated air. This drying method is simple and thus commonly used [4]. However, its efficiency is low [5]. In vacuum drying, the product is dried at sub-atmospheric pressure. Products dried using this method are generally of a better quality [6]. The synergistic combination of vacuum and hot air drying results in high-quality products with a short processing time and low power consumption. Maize can be effectively dried using a combination of the vacuum and hot air processes [7].

Foods are viscoelastic materials [8]. The data on viscoelastic behavior of foods can be used to describe processing operations [9]. The drying conditions, maize varieties, and ripening stage can affect the viscoelastic properties of maize kernel. Stress relaxation is an essential characteristic of a viscoelastic material [10]. In a stress relaxation experiment, a constant deformation is applied to the product and the decline in the stress over time to keep this deformation is measured [11]. Li et al. [12] found that the five-element Maxwell equation could predict the stress relaxation property of sweet potato better than the three-element Maxwell equation. Wang et al. [11] studied the stress relaxation property of rice.

They measured the relaxation modulus. Abedi and Takhar [13] investigated the stress relaxation behavior of banana. The ripening stage could affect the rheological behavior pattern of banana in the drying process.

Creep is another essential characteristic of a viscoelastic material [10]. In a creep experiment, a fixed force is applied to the product and the displacement is measured. Li et al. [12] performed the creep-recovery cycle test on sweet potato. They repeated the cycle three times. After the first cycle, no significant differences in the creep elements were observed. Ditudompo et al. [14] found that the Burgers' equation could describe the creep behavior of an extruded cornstarch well ($R^2 > 0.92$). Ozturk and Takhar [15] studied the viscoelastic behavior of carrot. The creep property of carrot was highly correlated with the moisture content. The storage of maize can be simulated by creep experiments [16]. However, it is difficult to conduct stress relaxation and creep experiments over a wide time range.

Prolonging the time and raising the temperature have an equivalent influence on the viscoelastic behavior of materials. This is known as the theory of time–temperature super-position (TTS) [17]. The applicable standards for TTS are as follows [18]: (a) neighboring curves can be joined to form a smooth curve; (b) all the viscoelastic functions must be super-imposed with an identical α_T; and (c) the relationship between α_T and temperature must satisfy the empirical equations. Polymers that follow TTS are called thermorheologically simple polymers; those that do not follow TTS are called thermorheologically complex polymers [19]. TTS has previously been tested in various polymers [11,20–25]. However, the application of TTS to maize kernel has not been reported.

The purposes of the current study were (i) to describe the viscoelastic behavior of maize kernel dried using a combination of vacuum and hot air processes; (ii) to assess the applicability of TTS to maize kernel; and (iii) to characterize the viscoelastic behavior of maize kernel over a wide timescale using TTS.

2. Materials and Methods

2.1. Materials

The variety of maize employed in this study was Nongda 86. Its seed kernels were obtained from freshly harvested maize (Beijing Sinong Seed Co., Ltd., Beijing, China) from Zhangye city, Gansu province, China. The kernels' initial water content was 27%. Prior to further testing, the kernels were kept in self-sealing bags and refrigerated at 4 °C.

2.2. Drying of Maize Kernels

The maize kernels were dried using the two methods detailed below. The samples' water content was determined using a GTR800E single-kernel moisture tester (Shizuoka Seiki Co., Ltd., Shizuoka, Japan).

2.2.1. Natural Drying (ND)

The maize kernels were placed on six glass plates (diameter: 20 cm) (Lanyi reagent company, Beijing, China) in one or two (thin) layers and then dried indoors to a water content of 13%. Finally, the samples were kept in self-sealing bags and refrigerated at 4 °C.

2.2.2. Hot Air/Vacuum Drying (HVD)

In a 50 °C oven (Shanghai Yiheng Scientific Instrument Co., Ltd., Shanghai, China), the maize kernels were firstly dried to a water content of 18%. Then, in a −0.1 MPa DZ-3 vacuum drier (Taisite Instrument Co. Ltd., Tianjin, China), the samples were separately dried at 75 °C, 65 °C, 55 °C, 45 °C, and 35 °C to a water content of 13%. Finally, the samples were kept in self-sealing bags and refrigerated at 4 °C.

2.3. Sample Preparation

To ensure the maize kernels had a flat and smooth surface, every sample was carefully polished by hand to prevent any physical failure caused by using abrasive papers. A

Fowler PRO-MAX digital vernier caliper (Newton, MA, USA) with a precision of 0.01 mm was employed to determine the width and length of every sample. The dimensions of the samples were about 9 mm × 4 mm × 4 mm (length × width × height). The sample preparation process was based on our previous research [26].

2.4. Stress Relaxation Tests

A TA Instruments Q800 dynamic mechanical analyzer (DMA, New Castle, DE, USA) was employed to measure the maize kernels' relaxation moduli. The compression mode was employed to carry out the tests. A 0.05 N preload was applied to ensure complete contact between the surface of the sample and the compression plate. The samples were equilibrated at four test temperatures (85 °C, 65 °C, 45 °C, and 25 °C) for 1 min. Then, the tests were conducted at the 0.8% strain for 10 min.

The generalized Maxwell equation (Equation (1)) was employed to describe the maize kernel relaxation modulus:

$$E(t) = \sum_{m=1}^{n} E_m \exp(-t/\tau_m) + E_0 \tag{1}$$

where $E(t)$ (MPa) and E_0 (MPa) denote the stress relaxation modulus and equilibrium modulus, respectively; τ_m (s) is the relaxation time; E_m (MPa) is the corresponding relaxation modulus; and t (s) is the time.

The Kohlrausch–Williams–Watts (KWW) equation (Equation (2)) was also employed to predict the modulus:

$$E(t) = E_0 \exp[-(t/\tau)^{\beta}] \tag{2}$$

where E_0 (MPa) denotes the initial modulus, τ (s) denotes the relaxation time, and β denotes the exponent.

2.5. Creep Tests

The DMA was also employed to determine the kernels' strains. The compression mode was employed to carry out the tests. A 0.05 N preload was supplied to each kernel. The samples were equilibrated at four test temperatures (60 °C, 50 °C, 40 °C, and 30 °C) for 1 min. Then, the tests were performed at 0.08 MPa stress for 10 min.

Burgers' equation (Equation (3)) was employed to predict the creep strain.

$$\varepsilon = \frac{\sigma}{E_1} + \frac{\sigma}{E_2}\left[1 - \exp\left(-t\frac{E_2}{\eta_2}\right)\right] + \frac{\sigma}{\eta_1}t \tag{3}$$

In Equation (3), t (s) represents time; ε (dimensionless) denotes the kernel's strain; σ (MPa) denotes the applied stress; η_1 (MPa s) and η_2 (MPa s) denote the Maxwell dashpot viscosity and Kelvin dashpot viscosity, respectively; and E_1 (MPa) and E_2 (MPa) denote the Maxwell spring modulus and Kelvin spring modulus, respectively. Generally, $\eta_2/E_2 = \tau$, where τ denotes the Kelvin element retardation time.

From the differentiation of Equation (3), the creep rate ε' can be acquired:

$$\varepsilon' = \frac{d\varepsilon}{dt} = \frac{\sigma}{\eta_1} + \frac{\sigma}{\eta_2}\exp\left(-t\frac{E_2}{\eta_2}\right) \tag{4}$$

When the time tends to infinity, ε' will gradually reach a certain value:

$$\varepsilon'(\infty) = \frac{d\varepsilon}{dt}\bigg|_{t=\infty} = \frac{\sigma}{\eta_1} \tag{5}$$

Another equation, called the Findley power law, can also describe the strain of polymers [27]. It has the following form:

$$\varepsilon = at^b + \varepsilon_0 \tag{6}$$

Here, ε_0 denotes the initial deformation, while a and b denote the material parameters.

A simpler two-parameter power law equation has also been employed to describe the strain of the polymers [28–30]:

$$\varepsilon = at^b \tag{7}$$

2.6. Time–Temperature Superposition

The strain and relaxation modulus of the maize kernels over a wide time range were described using TTS. The master curves were produced by transferring the short-period curves horizontally [31]. The William–Landel–Ferry (WLF) [19] (Equation (8)) or Arrhenius equation [32] (Equation (9)) can be employed to describe the shift factor.

$$\log \alpha_T = \frac{C_1 T_0 - C_1 T}{T - T_0 + C_2} \tag{8}$$

In Equation (8), α_T, T_0 (K), and T (K) represent the shift factor, reference temperature, and test temperature, respectively, while C_1 and C_2 (K) are the WLF parameters.

$$\log \alpha_T = \frac{E_a}{R}\left(\frac{1}{T} - \frac{1}{T_0}\right) \tag{9}$$

In Equation (9), R (J/K·mol) and E_a (kJ/mol) denote the gas law constant and activation energy, respectively, while T_0 (K) and T (K) denote the reference and experimental temperatures, respectively.

As suggested by Ferry [18], the Arrhenius equation and WLF equation were both employed to describe α_T. C_1, C_2, E_a, and the coefficient of determination (R^2) were determined from the experimental data using regression analysis. Temperatures of 25 °C and 30 °C were chosen as the reference temperatures for stress relaxation and creep TTS, respectively.

2.7. Statistical Analysis

Three replicates were conducted for every sample. Universal Analysis 2000 software (version 4.3A, TA Instruments, New Castle, DE, USA) was employed to acquire the DMA data. SPSS 17.0 (SPSS Inc., Chicago, IL, USA) was employed to conduct the statistical analysis.

3. Results and Discussion

3.1. Analysis of Stress Relaxation Behavior

The stress relaxation data for maize kernels at different temperatures are plotted in Figure 1. Three stages make up the curve. The first stage shows an immediate elastic response. The timescale of this region is nearly zero. The second stage demonstrates a marked stress relaxation process. The timescale is from about 0 to 20 s. In the third stage, the modulus approaches a constant. The maize kernel is viscoelastic [8]. When strain is applied to the kernel, the stress increases immediately due to the elastic portion of the kernel and then decreases gradually due to the viscous portion of the kernel. This trend is identical to the findings reported in a previous study [33]. It can be seen from Figure 1 that the kernels dried by ND had the highest initial relaxation modulus. This is because the kernels dried by ND had the highest toughness. For the same sample, when the temperature was increased, the initial modulus declined markedly. This was caused by an increase in the motion of the polymer chains, resulting in a lowering of the threshold for specific strain conditions [34].

Table 1 presents the elements of the generalized Maxwell equation. As listed in Table 1, the R^2 was around 0.94–0.98, indicating that the stress relaxation modulus was described well by the generalized Maxwell equation. A similar finding was reported in a study on oat grains [35]. Table 1 also shows that E_1 decreased as the temperature increased, suggesting that higher temperatures reduced the maize kernel's deformation resistance [36]. Hence, the stress required to achieve the given strain decreased. At the same temperature, τ fluctuated with drying conditions and did not display a decreasing or increasing tendency, suggesting that the relaxation time was not related to the drying method. In general, τ

decreased as the temperature increased. That is, kernels relaxed more rapidly at higher temperatures. The reason for this is as follows: when a maize kernel becomes soft due to high temperatures, the cell wall viscosity and polysaccharide tangles will be reduced, leading to faster stress dissipation [36]. By using the expression below, the Deborah number (D_e) can be obtained:

$$D_e = \tau / t \tag{10}$$

Here, *t* denotes the observation time. D_e can provide useful information on materials' viscoelastic properties: $D_e \approx 1$ denotes a viscoelastic behavior; $D_e \ll 1$ denotes a viscous fluid; and $D_e \gg 1$ denotes an elastic solid [37]. The D_e values (0.094–0.385) calculated in this study were much smaller than one; this suggests that the Maxwell element showed viscous behavior.
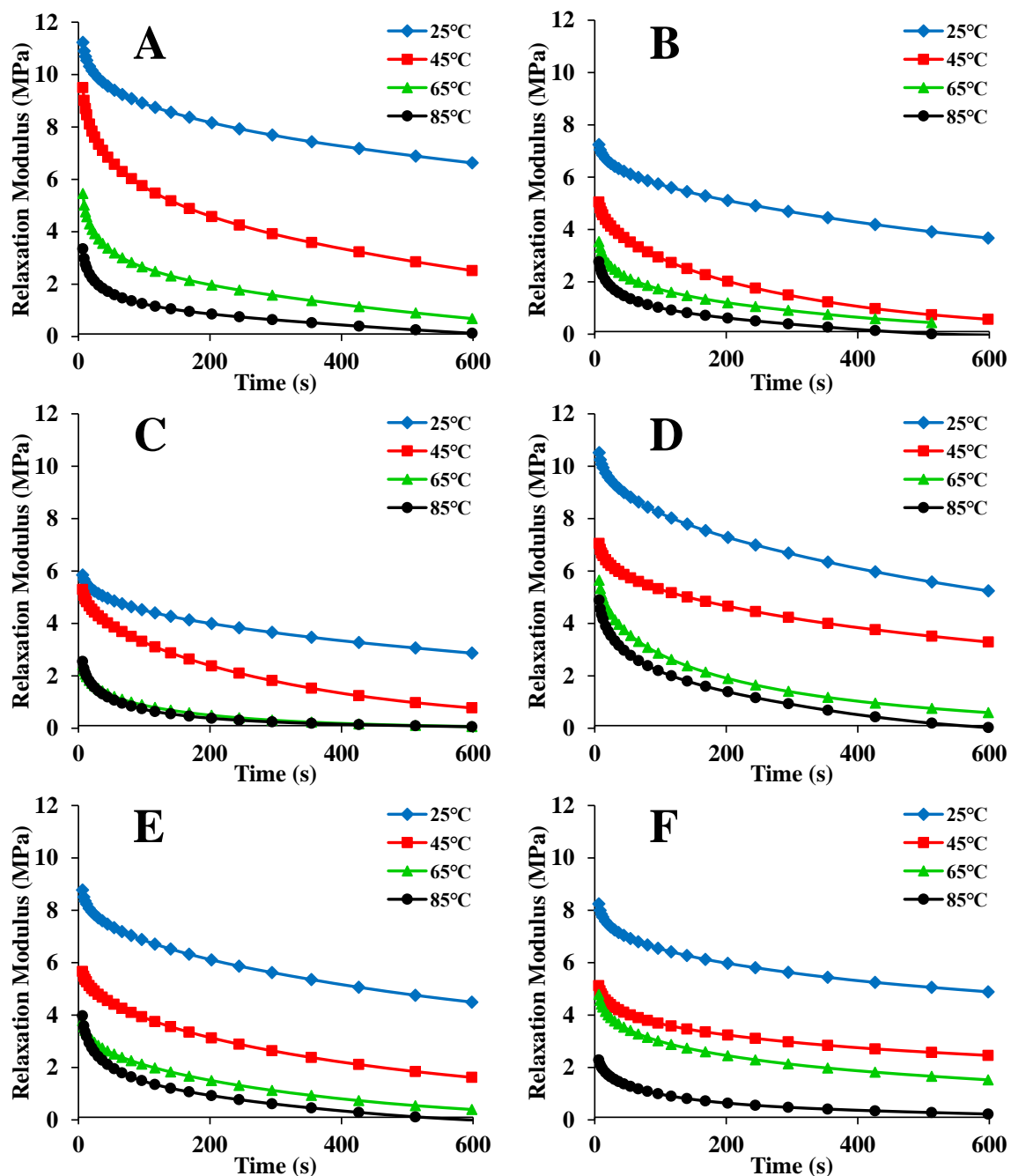

Figure 1. Relaxation modulus data for maize kernels at different temperatures: (**A**) natural drying (ND); (**B**) hot air/vacuum drying (HVD) 35 °C; (**C**) HVD 45 °C; (**D**) HVD 55 °C; (**E**) HVD 65 °C; (**F**) HVD 75 °C.

Table 1. Parameters of the generalized Maxwell equation for maize kernels.

Drying Condition	T (°C)	E_1 (MPa)	τ (s)	E_0 (Mpa)	R^2
ND	25	3.893	155.324	6.894	0.970
	45	5.934	127.648	3.024	0.973
	65	3.855	101.195	1.150	0.960
	85	2.580	70.449	0.502	0.949
HVD 35 °C	25	3.349	231.258	3.609	0.982
	45	4.180	168.697	0.631	0.989
	65	2.265	122.905	0.674	0.971
	85	2.337	87.183	0.203	0.964
HVD 45 °C	25	2.715	198.521	2.915	0.982
	45	4.308	194.858	0.738	0.990
	65	2.045	82.344	0.208	0.977
	85	2.237	56.494	0.225	0.976
HVD 55 °C	25	4.893	211.059	5.252	0.983
	45	3.368	187.663	3.374	0.980
	65	4.495	118.842	0.866	0.984
	85	4.144	119.810	0.359	0.973
HVD 65 °C	25	3.896	206.480	4.516	0.981
	45	3.848	204.399	1.597	0.989
	65	2.994	163.361	0.506	0.980
	85	3.269	86.022	0.364	0.962
HVD 75 °C	25	2.867	154.009	5.058	0.974
	45	2.260	129.410	2.635	0.974
	65	2.791	124.449	1.743	0.976
	85	1.803	87.104	0.367	0.980

Table 1 also shows that when the temperature increased, E_0 decreased. This suggests that maize kernel is mainly a viscous material at high temperatures. The maize kernel's viscous portion begins to decrease as the temperature decreases. According to the theory of free volume, molecular dynamics can account for the influence of the viscous portion. When the temperature is low, there is not enough free volume to allow for the motion of molecular chains; thus, the molecules' movement is fixed. This makes the kernel glassy. When the temperature is high, the free volume becomes larger and the molecular chains can move. This makes the kernel rubbery [11]. In addition, the E_0 for ND was higher than the E_0 for HVD (at the same temperature), except in the case of HVD 55 °C at 45 °C and HVD 75 °C at 65 °C. This suggests that the kernel's stiffness changed. This is owing to the changes in the kernel's cellular structure caused by hot air/vacuum drying, giving rise to a decline in the stiffness. The change in E_0 may have resulted from the breakdown of cell membranes caused by HVD [38], leading to the collapse of the cells [33,39].

3.2. Analysis of Creep Behavior

Figure 2 displays the creep curves for maize kernels at various temperatures. The curves demonstrate classic creep features and exhibit a similar tendency over time. When stress is applied to the maize kernels, the strain increases instantly because of elasticity. In this portion, the changes in the kernel's structure are reversible [40]. Then, the strain continues to increase at a decreasing rate due to viscosity. This portion of the curve contributes to the maize kernel's viscoelastic property [15]. The last portion is a straight line, representing the kernel's viscous flow deformation. In this compression stage, the kernel's tissues are permanently destroyed, and the changes can only be partially reversed [41]. This tendency is consistent with the creep strain of barley kernels reported in a previous study [42]. In this study, the creep strain exhibited a strong temperature dependence. When the temperature increased, the strain also increased. A similar finding was reported in a previous study [43]. Therefore, the solid-like characteristics of maize kernel increase as the temperature decreases [14]. It can also be seen from Figure 2 that the ND kernels had

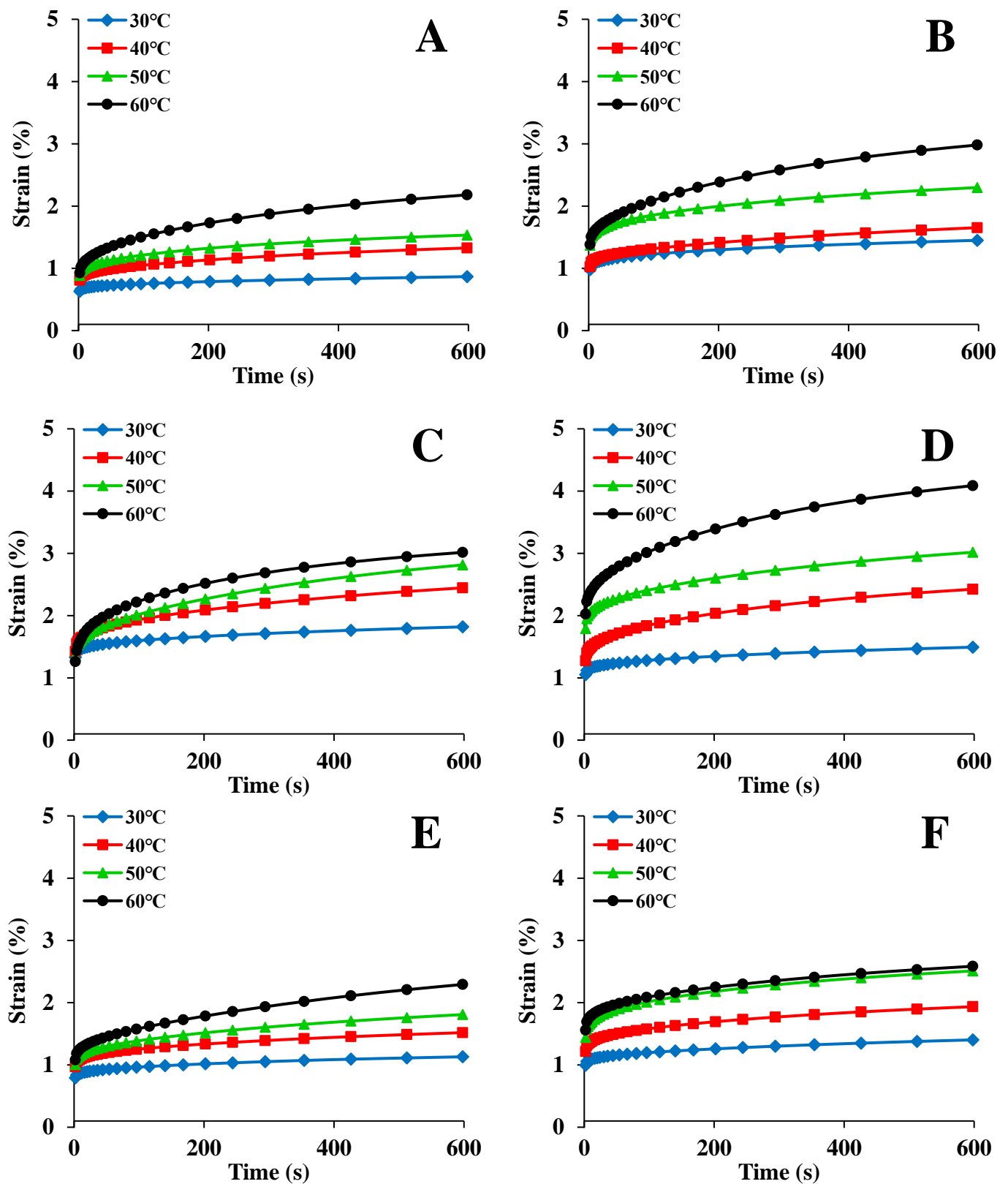the lowest creep strain. This is because the kernels dried using the ND method were more compact and robust.

Figure 2. Creep data for maize kernels at different temperatures: (**A**) ND; (**B**) HVD 35 °C; (**C**) HVD 45 °C; (**D**) HVD 55 °C; (**E**) HVD 65 °C; (**F**) HVD 75 °C.

Table 2 displays the values of the four elements (E_1, E_2, η_1, and η_2) mentioned in Section 2.5. The data in this table suggest that Burgers' equation can predict the creep property well ($R^2 > 0.98$). E_1, E_2, η_1, and η_2 all decreased as the temperature increased, suggesting that increasing temperature increases the deformation of maize kernel. E_1 is correlated with the elasticity of a semi-crystalline polymer's crystalline regions. In contrast to the amorphous zones, the crystalline regions are exposed to instant stress because of their relatively high hardness. When the stress is eliminated, E_1 can be resumed instantly [44]. E_2 is correlated with the rigidity of a material [30]. When the temperature increases, the instant and viscoelastic strain increase. As a result, E_1 and E_2 decrease. η_1 is correlated with the damage from the crystalline regions and the irrevocable strain from the amorphous zones. η_2 corresponds to the viscosity of the semi-crystalline polymer's amorphous zones [45]. When the temperature increases, the values of η_1 and η_2 decline. This indicates that the molecular chains become more active [29]. The ND elements exhibited the greatest declines (particularly in η_1, which depends heavily on temperature and is correlated with the rate of long-period deformation), suggesting that the viscoelastic property of kernel dried by ND was more sensitive to temperature.

Table 2. Parameters of Burgers' equation for maize kernels.

Drying Condition	T (°C)	E_1 (MPa)	E_2 (MPa)	η_2 (MPa s)	η_1 (MPa s)	τ (s)	ε' (∞) ($\times 10^{-6}$ s^{-1})	R^2
ND	30	12.366	93.513	2123.752	3.343×10^4	22.711	2.393	0.986
	40	9.459	44.621	1960.307	1.500×10^4	43.932	5.335	0.991
	50	8.550	29.893	1429.997	1.362×10^4	47.837	5.874	0.991
	60	8.037	15.943	884.383	6667.172	55.472	11.999	0.995
HVD 35 °C	30	7.874	44.399	1249.639	1.758×10^4	28.146	4.551	0.986
	40	7.510	39.770	1249.193	1.169×10^4	31.410	6.846	0.991
	50	5.546	21.809	782.902	9165.199	35.898	8.729	0.989
	60	5.392	12.599	869.341	5301.574	69.001	15.090	0.995
HVD 45 °C	30	5.860	42.303	822.937	1.662×10^4	19.453	4.813	0.982
	40	5.346	21.779	685.719	7719.949	31.485	10.363	0.990
	50	5.511	15.600	752.968	5336.196	48.267	14.992	0.993
	60	5.858	9.698	377.393	5333.766	38.915	14.999	0.990
HVD 55 °C	30	7.352	50.190	1277.306	1.815×10^4	25.449	4.409	0.985
	40	5.876	18.000	778.471	7273.839	43.248	10.998	0.991
	50	4.255	18.021	530.068	6427.004	29.414	12.447	0.988
	60	3.671	9.550	512.969	4199.839	53.714	19.048	0.992
HVD 65 °C	30	9.741	65.245	2054.107	2.380×10^4	31.483	3.361	0.987
	40	7.926	39.079	1085.328	1.463×10^4	27.773	5.467	0.987
	50	7.549	28.880	1011.784	9554.119	35.034	8.373	0.991
	60	6.956	22.999	957.637	5738.029	41.638	13.942	0.994
HVD 75 °C	30	7.816	57.858	1335.159	1.856×10^4	23.076	4.311	0.986
	40	6.288	30.236	975.934	1.119×10^4	32.277	7.149	0.988
	50	5.263	18.040	602.605	8122.873	33.404	9.849	0.988
	60	4.896	20.384	621.951	7975.713	30.512	10.030	0.988

It can also be seen from Table 2 that E_2 was larger than E_1. In comparison to the viscous and retarded elastic strain, the instant strain was larger. Thus, the Hookean spring elastic portion mainly makes up maize kernel's creep strain [14]. Table 2 also presents ε' (∞) and τ for the maize kernels. When the temperature was increased, ε' (∞) increased monotonically. At 60 °C, the kernels generally showed a longer retardation time (τ), indicating that the samples' viscoelastic property remained for longer [41].

Overall, the kernel dried by ND had a higher stiffness. The viscoelastic property of the kernel dried by ND was more sensitive to temperature. The relaxation time of the kernel was not related to the drying method.

3.3. Applicability of Time-Temperature Superposition

Figures 1 and 2 were replotted in logarithmic form (left-hand graphs in Figures 3 and 4) to employ TTS. It can be seen that for stress relaxation, the impact of temperature was obvious at 45 °C and became more significant at 65 °C; for creep, the impact was obvious at 50 °C and became significant at 60 °C. The temperature range of 45–65 °C and 50–60 °C denoted the order–disorder transformation zones of maize kernel [46]. These are close to the gelatinization temperature of maize starch (64–72 °C) [47]. Furthermore, from the graphs on the left in Figure 3, it can be seen that the long relaxation behavior became obvious when the temperature was above 45 °C. Specific molecular interactions in maize kernel and temperature have an impact on when the long relaxation process occurs [21]. In general, in this study, long relaxation occurred when the time was approximately 200 s at 65 °C, and when it was 160 s at 85 °C. This is because the hydrogen bonds were weakened when the temperature was raised [48].
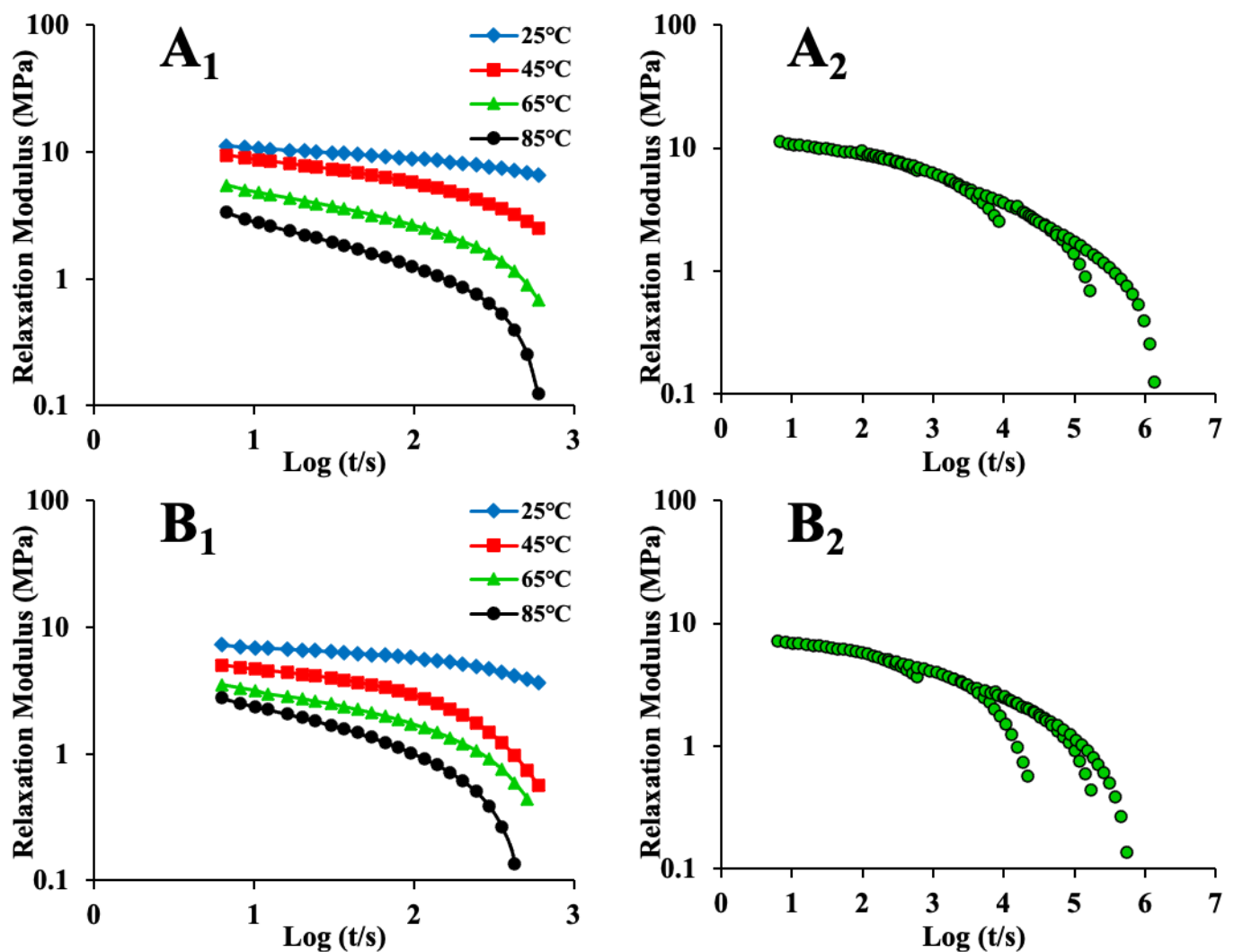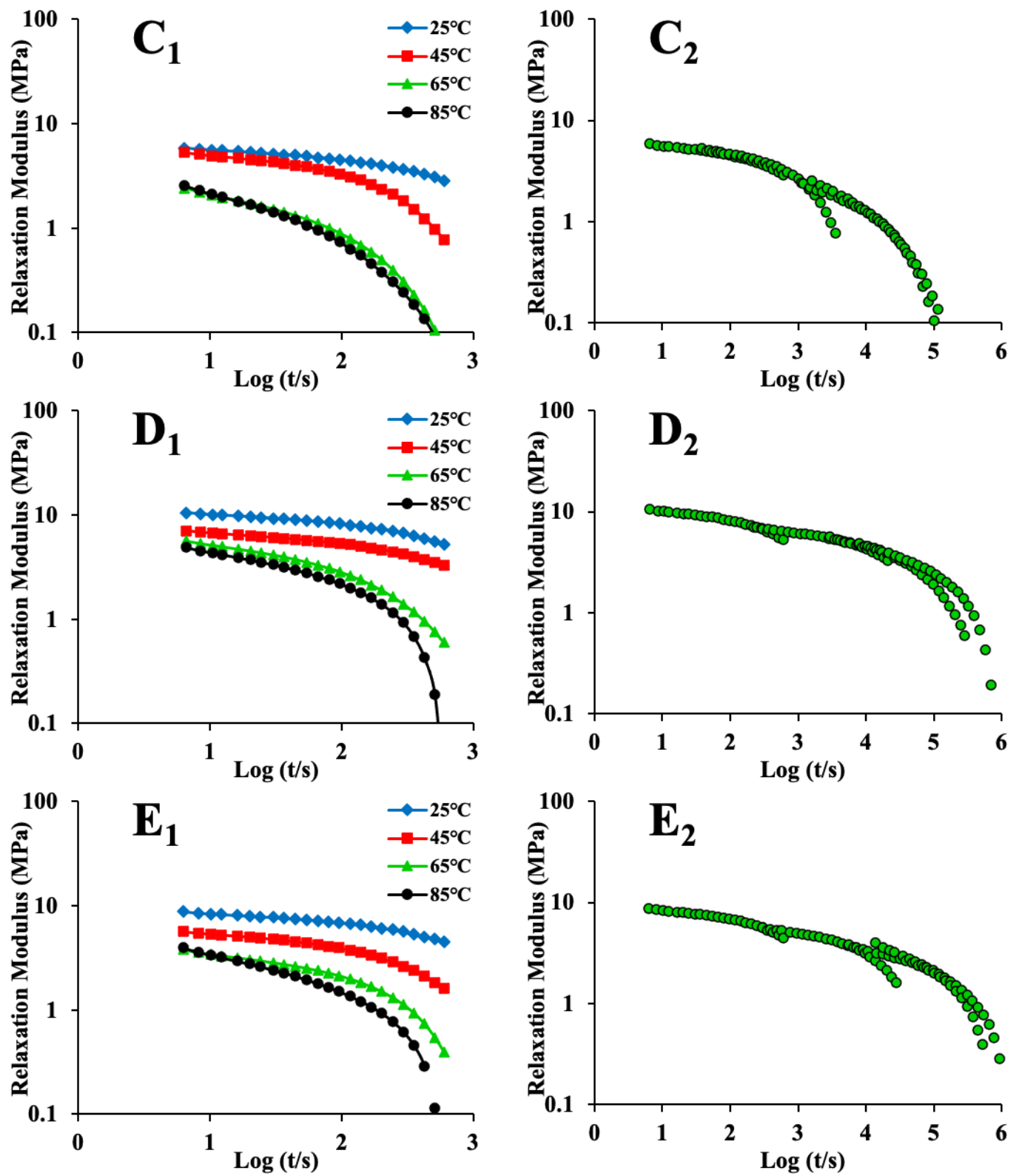

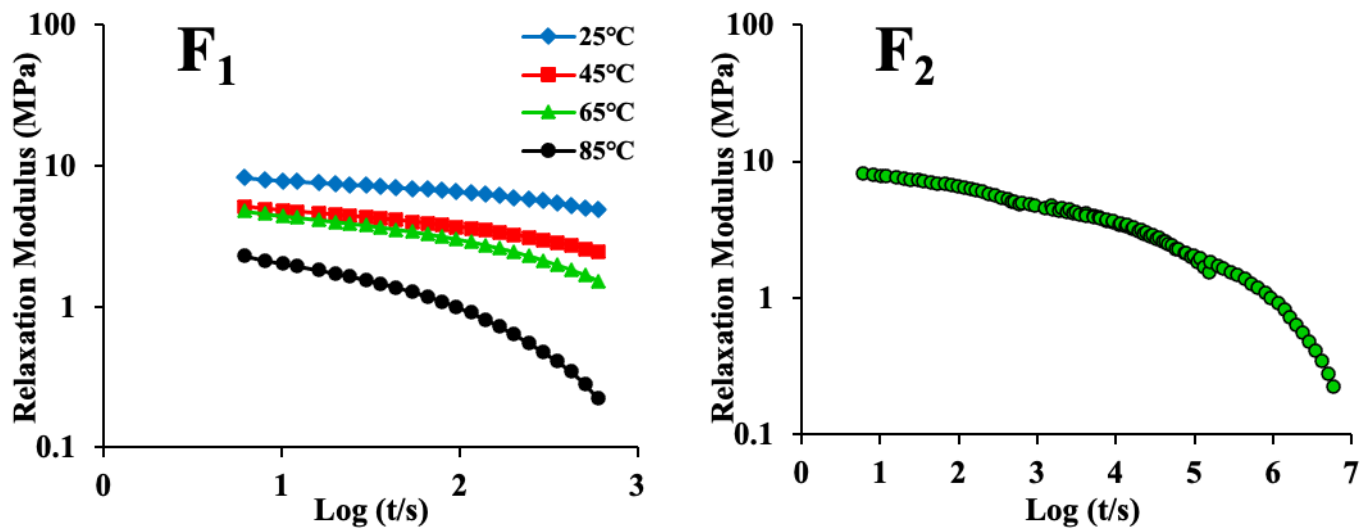
Figure 3. *Cont.*

Figure 3. *Cont.*

Figure 3. The left-hand graphs show logarithmic plots of stress relaxation data for maize kernels, while the right-hand graphs are the corresponding master curves for maize kernels (A_1,A_2)—ND; (B_1,B_2)—HVD 35 °C; (C_1,C_2)—HVD 45 °C; (D_1,D_2)—HVD 55 °C; (E_1,E_2)—HVD 65 °C; (F_1,F_2)—HVD 75 °C.
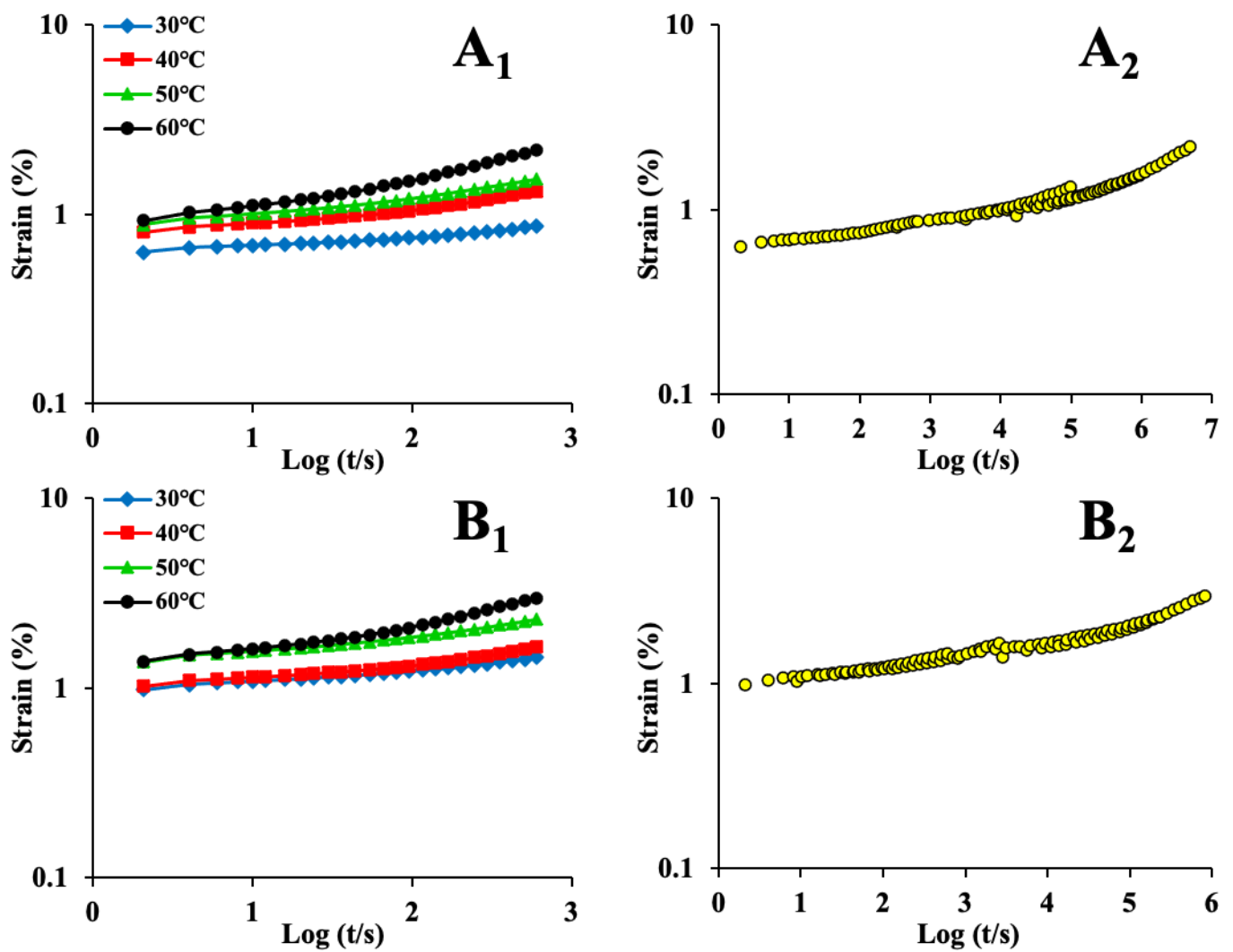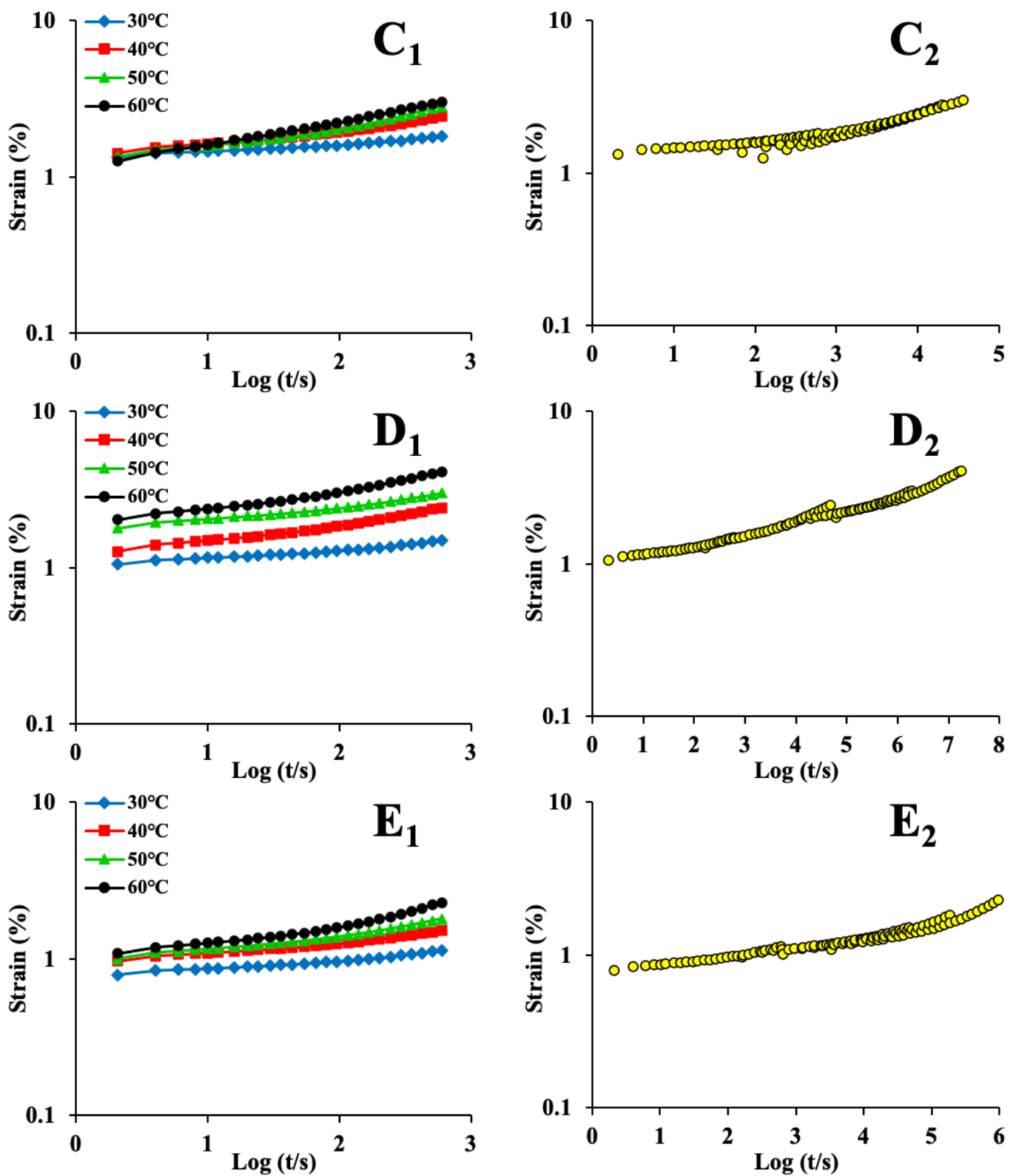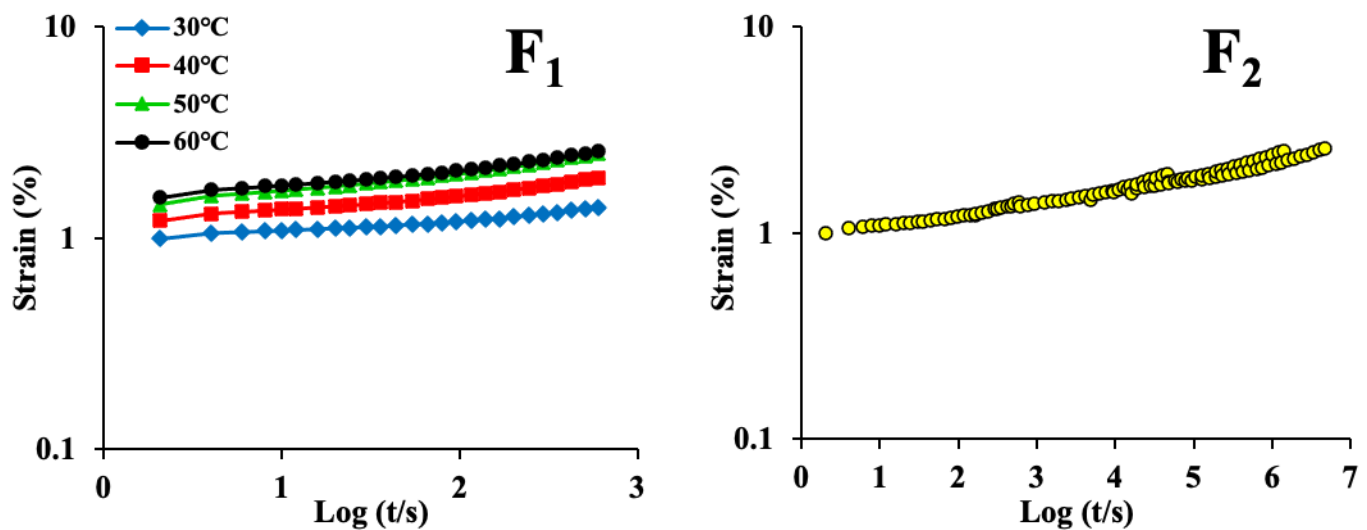

Figure 4. *Cont*.

Figure 4. *Cont.*

Figure 4. The left-hand graphs show logarithmic plots of creep data for maize kernels, while the right-hand graphs are the corresponding master curves for maize kernels (A_1,A_2)—ND; (B_1,B_2)—HVD 35 °C; (C_1,C_2)—HVD 45 °C; (D_1,D_2)—HVD 55 °C; (E_1,E_2)—HVD 65 °C; (F_1,F_2)—HVD 75 °C.

By shifting the stress relaxation (left-hand graphs in Figure 3) and creep (left-hand graphs in Figure 4) curves horizontally, the master curves were acquired (right-hand graphs in Figures 3 and 4). As noted earlier, the applicable standards for TTS are as follows: (a) neighboring curves can be joined to form a smooth curve; (b) all the viscoelastic functions must be superimposed with an identical α_T; and (c) the relationship between α_T and the temperature must satisfy the empirical equations. It can be seen from the graphs in Figures 3 and 4 (right) that the relaxation and creep curves exhibited superposition for all the samples, although the master curves showed some tails and irregularities (Figure 3(A_2–E_2) and Figure 4(B_2,C_2)). The absence of superposition is correlated with the relaxation mechanism, which depends on temperature and takes place inside the maize kernel [49]. This is parallel to the findings reported in a previous study [50]. In that study, the curves obtained at higher temperatures could not be overlapped smoothly with only horizontal shifting. Nevertheless, by shifting the obtained curves both vertically and horizontally, smooth master curves were acquired. In general, the relaxation modulus and creep strain master curves were considered to be continuous and smooth in this study. Some curves (Figure 3(F_2) and Figure 4(A_2,D_2–F_2)) demonstrated an excellent fit for the TTS. These findings suggest that the maize kernel is a thermorheologically simple material [51]. The applicability of TTS has also been evaluated for other food materials [46,49,52–54], and soybean [55] was reported as a thermorheologically simple material.

It can be seen from Figures 5 and 6 that α_T reduced monotonically with the temperature. This is similar to the finding of Meza et al. [56]. Furthermore, α_T versus the temperature data could be fitted well by both the Arrhenius equation and the WLF equation ($R^2 > 0.857$). However, the correlation between α_T and the temperature was not very high for some samples. This is because the temperatures were too close, and no remarkable viscoelastic variations were detected, similar to the finding reported by Ahmed [49]. In his study, no noticeable rheological variations were found in guar gum dispersions due to the closeness of the temperatures.
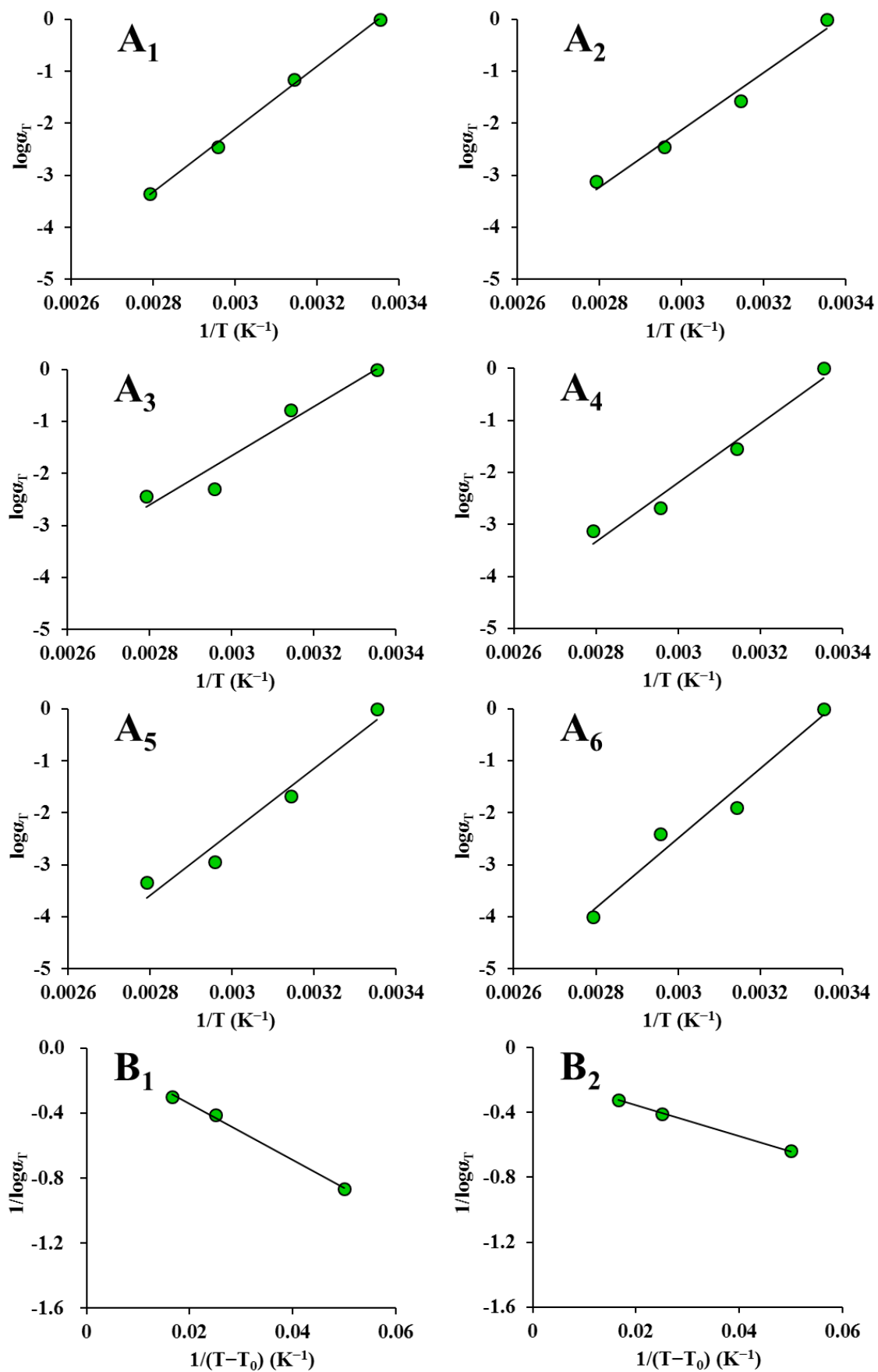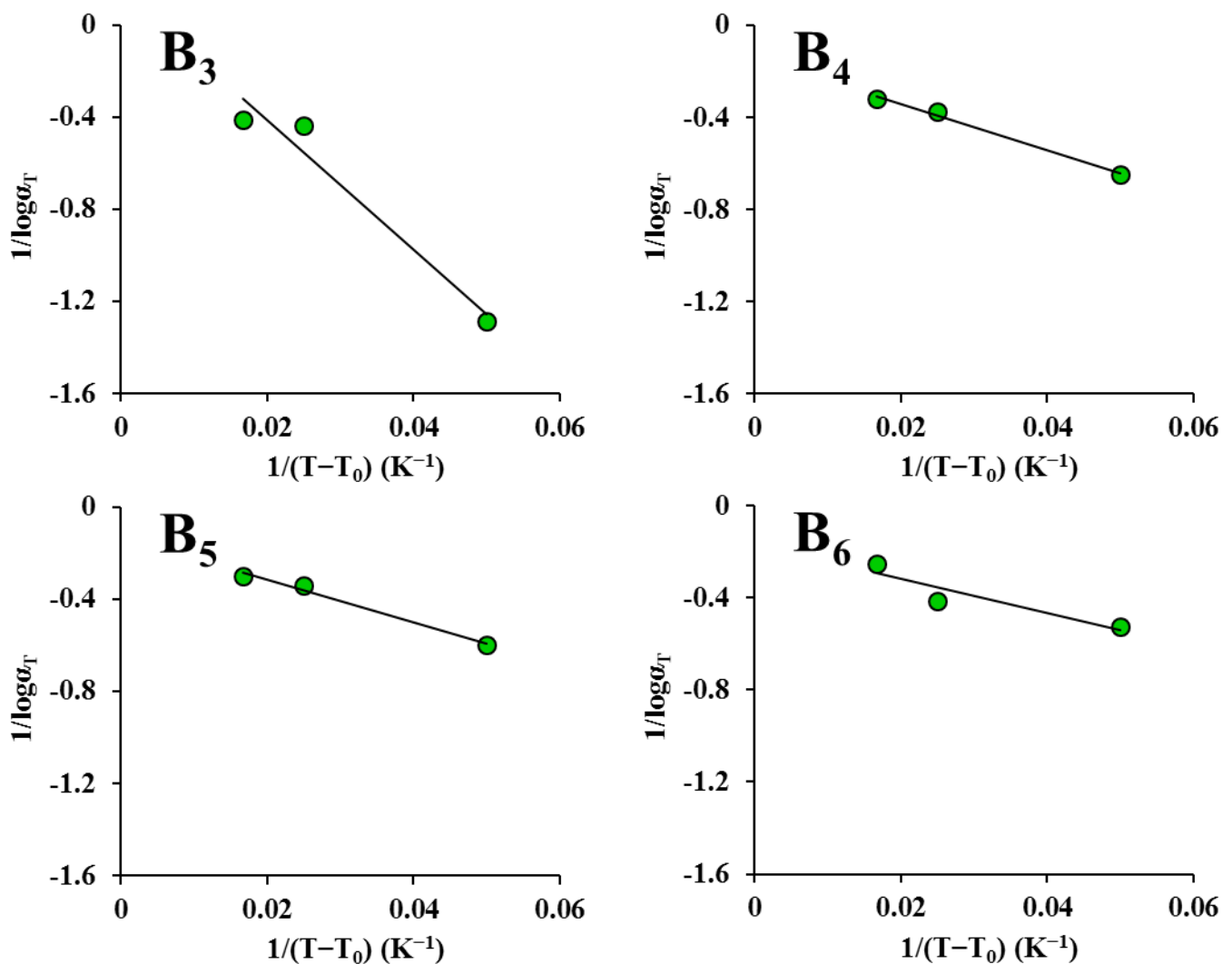
Figure 5. *Cont.*

Figure 5. Shift factors fitted to the Arrhenius equation for maize kernels (stress relaxation): (A_1) ND; (A_2) HVD 35 °C; (A_3) HVD 45 °C; (A_4) HVD 55 °C; (A_5) HVD 65 °C; (A_6) HVD 75 °C. Shift factors fitted to the William–Landel–Ferry (WLF) equation for maize kernels (stress relaxation): (B_1) ND; (B_2) HVD 35 °C; (B_3) HVD 45 °C; (B_4) HVD 55 °C; (B_5) HVD 65 °C; (B_6) HVD 75 °C.

Tables 3 and 4 display the Arrhenius activation energy (E_a) and WLF constants. The WLF constants, C_1 and C_2, are given by [57]:

$$C_1 = \frac{B}{2.303f} \tag{11}$$

$$C_2 = \frac{f}{\alpha} \tag{12}$$

Here, B can be taken equal to unity, f denotes the fractional free volume at the reference temperature, and α denotes the thermal expansion coefficient. Although the WLF constants fluctuated with the drying conditions, the WLF constants for ND and HVD 35 °C were the highest, suggesting that the fractional free volume and thermal expansion coefficient were the smallest.
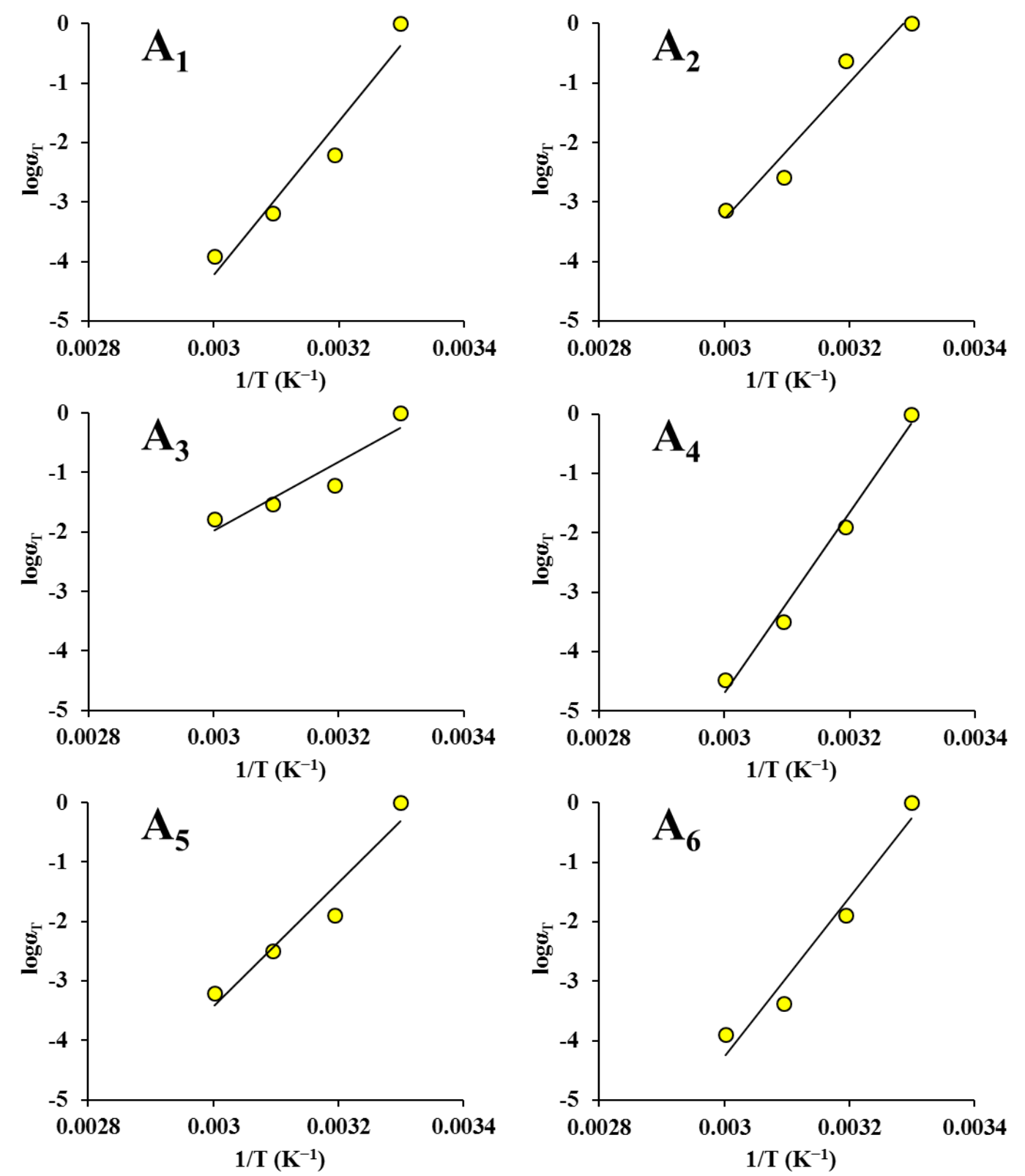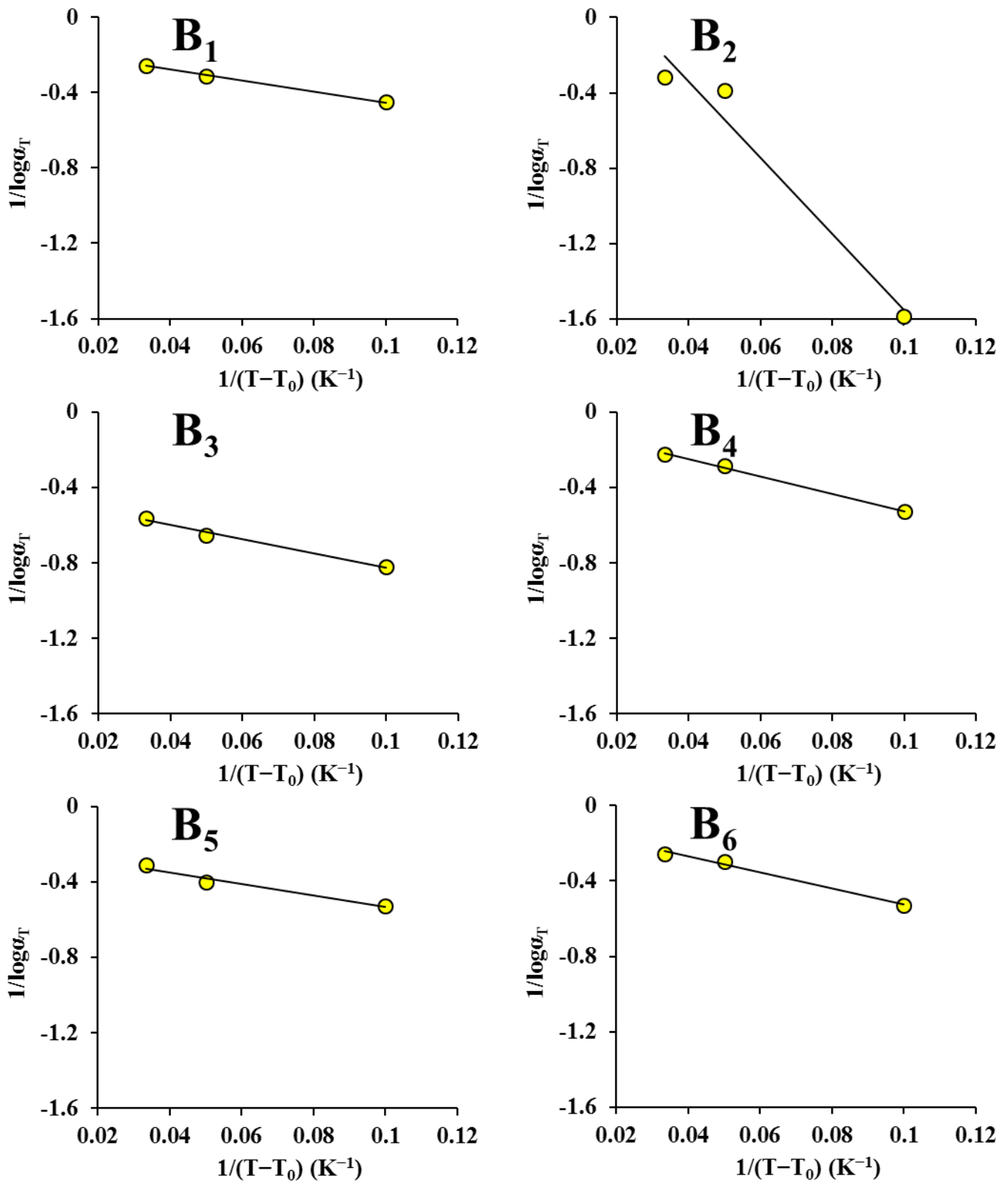
Figure 6. *Cont.*

Figure 6. Shift factors fitted to the Arrhenius equation for maize kernels (creep): (**A₁**) ND; (**A₂**) HVD 35 °C; (**A₃**) HVD 45 °C; (**A₄**) HVD 55 °C; (**A₅**) HVD 65 °C; (**A₆**) HVD 75 °C. Shift factors fitted to the WLF equation for maize kernels (creep): (**B₁**) ND; (**B₂**) HVD 35 °C; (**B₃**) HVD 45 °C; (**B₄**) HVD 55 °C; (**B₅**) HVD 65 °C; (**B₆**) HVD 75 °C.

Table 3. WLF constants and Arrhenius activation energy for maize kernels (stress relaxation).

Equation	Parameters	Drying Condition					
		ND	HVD 35 °C	HVD 45 °C	HVD 55 °C	HVD 65 °C	HVD 75 °C
WLF	C_1	14.990	5.995	8.406	7.174	7.758	5.882
	C_2 (K)	191.700	56.655	134.400	72.001	71.984	43.807
	R^2	0.997	0.999	0.953	0.992	0.986	0.857
Arrhenius	E_a	126.900	124.200	90.860	117.300	126.600	134.800
	R^2	0.997	0.959	0.934	0.967	0.960	0.963

Table 4. WLF constants and Arrhenius activation energy for maize kernels (creep).

Equation	Parameters	Drying Condition					
		ND	HVD 35 °C	HVD 45 °C	HVD 55 °C	HVD 65 °C	HVD 75 °C
WLF	C_1	6.127	32.020	2.226	15.873	4.435	9.671
	C_2 (K)	17.771	257.500	8.346	73.297	13.647	40.668
	R^2	0.998	0.963	0.985	0.998	0.966	0.989
Arrhenius	E_a	250.599	220.498	111.035	292.645	199.302	255.960
	R^2	0.932	0.945	0.870	0.987	0.936	0.955

It can be seen that the R^2 of the WLF equation was higher than that of the Arrhenius equation. A similar finding was reported in a previous study [58]. Despite this, it should be noted that there are two coefficients in the WLF equation, while there is only one coefficient in the Arrhenius equation. Hence, the WLF equation is more adaptable. We can also observe from Tables 3 and 4 that the C_1 and C_2 values ranged from 2.226 to 32.020 and 8.346 to 257.500 K, respectively. The values of C_1 were slightly different from the universal value (C_1 = 17.44), while the values of C_2 were considerably different (C_2 = 51.6 K) [57]. This is due to the complexity of food polymers (including different charges on the surfaces of polymers, various polysaccharides, 20 amino acids of protein, large polydispersities) [59] and is similar to the finding of Altay and Gunasekaran [60]. In their research, the values of C_1 and C_2 for a gelatin–xanthan gum system ranged from 4.52 to 22.68 and 58.97 to 204.97 K, respectively. Peleg [61] stated that employing universal values in food polymers ought to be approached cautiously. The values of C_1 and C_2 for food materials should be ascertained through experiments due to their substance-specific characteristics [59].

In this study, the E_a values for stress relaxation ranged from 90.86 to 134.8 kJ/mol. These values are very close to the E_a value (94.3 kJ/mol) of rice kernels (13.8% moisture content) for stress relaxation [11]. This is likely because maize kernels and rice kernels are both mainly composed of starch. The values for creep ranged from 111.035 to 292.645 kJ/mol, which are higher than the values (62.960–166.539 kJ/mol) for starch films [62,63]. Furthermore, the values for creep were significantly higher than those for stress relaxation. The E_a for relaxation and creep represents the energy needed for the initiation of the molecular movements, leading to relaxation and creep [64]. From Tables 3 and 4, the values for the kernels dried by HVD at 75 °C and HVD at 55 °C were the highest, suggesting that more energy was required, while the values for the kernels dried by HVD at 45 °C were the lowest.

Overall, TTS was successfully applied to the maize kernel. TTS extended the timescale of the relaxation modulus and creep strain from 2 to 5–6 log periods (Figure 3) and 2 to 4–7 log periods (Figure 4), respectively. Performing a DMA experiment for such a long time is extremely challenging. The application of TTS to the rice kernel was reported in a previous study [11]. In that study, the timescale of the relaxation modulus for the rice kernel was extended from 2 to 6 log periods.

3.4. Long-Period Stress Relaxation and Creep Response

Figure 7 shows the TTS predicted relaxation moduli for maize kernels dried under different conditions at 25 °C. As shown in this figure, the resulting predicted curves provide an accelerated stress relaxation characterization up to 1600 h. Constant strain-rate tests performed for yellow-dent maize kernels were reported in a previous study [9]. In that study, the timescale of the relaxation modulus was extended to 10^6 s; however, the modulus was higher than that in the current study. This may have resulted from differences in the maize varieties and experimental conditions.
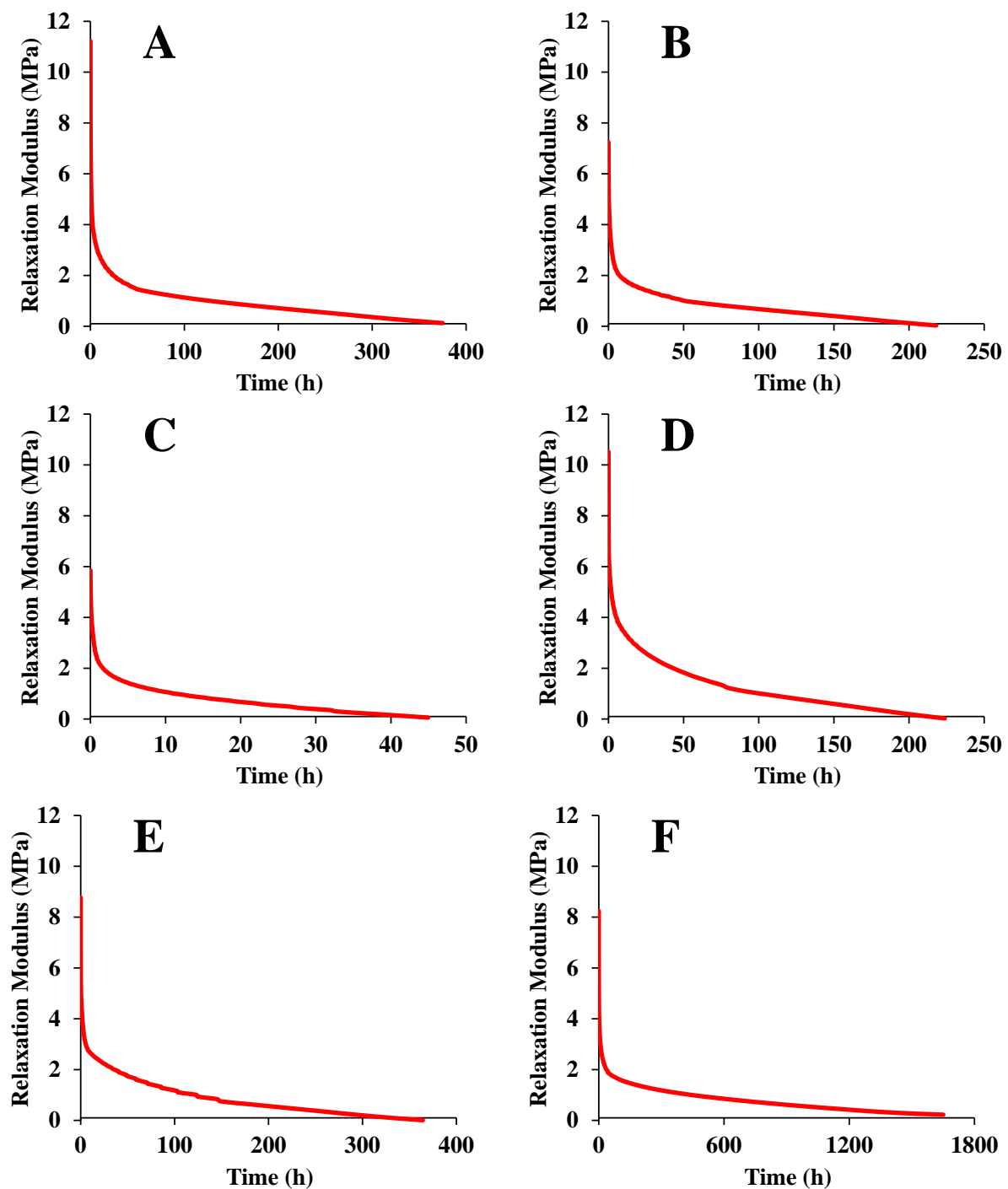

Figure 7. Time-temperature superposition (TTS) predicted stress relaxation for maize kernels dried under different conditions: (**A**) ND; (**B**) HVD 35 °C; (**C**) HVD 45 °C; (**D**) HVD 55 °C; (**E**) HVD 65 °C; (**F**) HVD 75 °C.

Figure 8 shows the TTS predicted creep strains for maize kernels dried under different conditions at 30 °C. The timescale of the creep strain was extended to 5000 h, and the trends of the curves were similar in the longer time frame. The timescale of the creep strain for the starch film was extended to 10^7 s in another study [63].
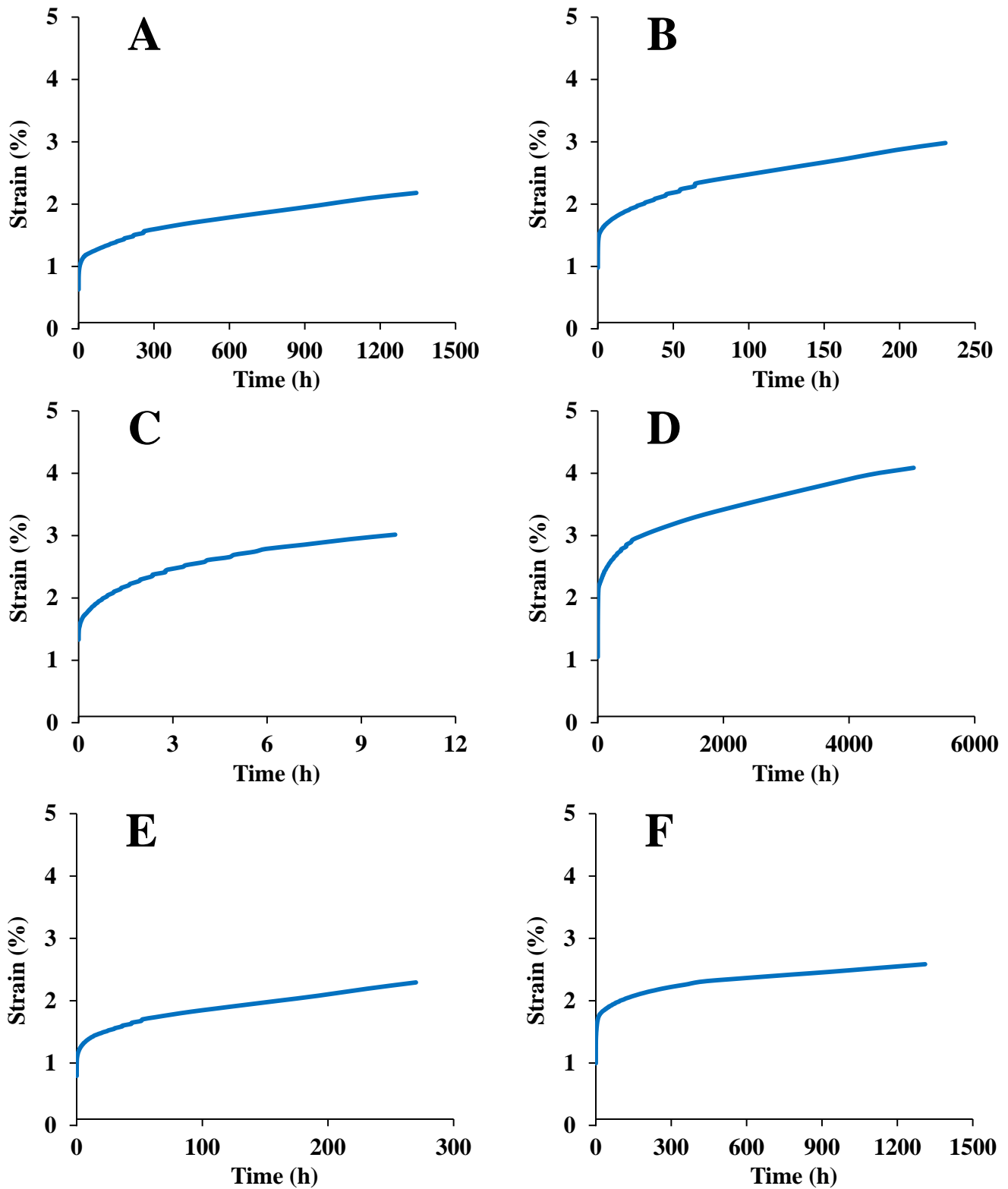

Figure 8. TTS predicted creep for maize kernels dried under different conditions: (**A**) ND; (**B**) HVD 35 °C; (**C**) HVD 45 °C; (**D**) HVD 55 °C; (**E**) HVD 65 °C; (**F**) HVD 75 °C.

Table 5 lists the equation parameters for long-period stress relaxation. We can observe from this table that both the Maxwell equation and KWW equation fitted the data well. The R^2 of the Maxwell equation was slightly higher than that of the KWW equation. Similar studies have reported fitting the generalized Maxwell equation to the relaxation modulus data of corn kernels [9] and rice kernels [11]. In this study, the values of E_1, E_2, and E_3 were close to each other. This suggests that the maize kernel's inner structure changed slightly during the long-period relaxation [36]. Furthermore, for the entire relaxation time, the Deborah numbers ($D_{e1} = 0.00034–0.14918$; $D_{e2} = 0.00004–0.21343$; $D_{e3} = 0.00011–0.06139$) were much smaller than one. This suggests that the first, second, and third Maxwell elements all show a viscous response.

Table 5. Equation parameters for long-period stress relaxation of maize kernels.

Equation	Parameters	Drying Condition					
		ND	HVD 35 °C	HVD 45 °C	HVD 55 °C	HVD 65 °C	HVD 75 °C
Generalized Maxwell equation	E_1 (MPa)	4.449	2.543	1.118	2.326	2.297	1.753
	E_2 (MPa)	2.802	1.796	1.674	3.555	2.763	3.166
	E_3 (MPa)	2.858	2.573	2.923	4.050	3.253	2.485
	τ_1 (s)	2177.795	4704.469	55.148	8945.749	5866.535	8.865×10^5
	τ_2 (s)	123.826	1.676×10^5	2.760×10^4	1.604×10^5	2.716×10^5	242.832
	τ_3 (s)	8.286×10^4	155.342	821.170	143.129	146.080	2.284×10^4
	E_0 (MPa)	0.668	0.095	0.095	0.322	0.172	0.365
	R^2	0.994	0.980	0.990	0.992	0.987	0.996
Kohlrausch–Williams–Watts (KWW) equation	E_0 (MPa)	16.501	10.670	7.847	13.554	14.006	12.593
	τ	1059.509	958.363	798.541	3888.804	791.291	1602.291
	β	0.194	0.191	0.271	0.187	0.149	0.145
	R^2	0.992	0.978	0.984	0.974	0.978	0.995

The value of the exponent β declined from 0.194 to 0.145 when the drying temperature was increased to 75 °C, except in the case of HVD at 45 °C. In accordance with Ngai et al.'s coupling theory [65], the medium and the relaxing species become more tightly coupled when β declines. This is correlated with overall declines in the molecular motion and increases in the width of the relaxation spectrum. The decline in β results from the increase in the density of the polymer with increasing drying temperature. When the space among the molecules is reduced, the motion of molecular chains is more limited, increasing the width of the relaxation spectrum [66].

Table 6 lists the equation parameters for long-period creep. We can observe from this table that the creep data were described well by Burgers' equation for all the maize kernels. Nonetheless, long-term experiments have considerably different elements than short-term experiments, caused by fitting a higher rate of creep to the strain in the short-term experiments [29].

Table 6. Equation parameters for long-period creep of maize kernels.

Equation	Parameters	Drying Condition					
		ND	HVD 35 °C	HVD 45 °C	HVD 55 °C	HVD 65 °C	HVD 75 °C
Burgers equation	E_1 (MPa)	10.244	6.968	5.251	6.081	8.161	6.503
	E_2 (MPa)	17.795	13.754	11.929	7.081	18.004	11.459
	η_2 (MPa s)	4.317×10^5	2.145×10^4	3.291×10^4	1.142×10^5	1.789×10^5	1.821×10^5
	η_1 (MPa s)	3.389×10^7	4.294×10^6	3.126×10^5	6.964×10^7	8.018×10^6	4.386×10^7
	R^2	0.951	0.956	0.966	0.950	0.946	0.922
Two-parameter power law equation	a	0.005	0.008	0.010	0.008	0.006	0.009
	b	0.088	0.083	0.097	0.088	0.080	0.067
	R^2	0.905	0.932	0.970	0.879	0.912	0.970
Findley power law equation	a	2.418×10^{-4}	0.001	2.829×10^{-4}	0.003	4.020×10^{-4}	0.003
	b	0.263	0.254	0.392	0.148	0.254	0.113
	ε_0	0.007	0.010	0.014	0.008	0.008	0.007
	R^2	0.978	0.977	0.974	0.982	0.974	0.976

The Findley power law equation can better represent the TTS predicted strain than Burgers' equation. The two-parameter power law equation also describes the creep data

well. When the parameter ε_0 was removed, *a* and *b* became more consistent. This is similar to the finding from a previous study [19].

4. Conclusions

With regard to stress relaxation, creep, and TTS, the rheological properties of maize kernels dried using a combination of vacuum and hot air processes were investigated. The kernel dried by ND had a higher stiffness. The viscoelastic property of kernel dried by ND was more sensitive to temperature. The relaxation time of the kernel was not related to the drying method. The long relaxation behavior became obvious when the temperature was above 45 °C, as a result of the weakening of hydrogen bonds with temperature. The D_es were all much smaller than one, indicating that the Maxwell elements showed viscous behavior. The maize kernels exhibited dominant viscous behavior at high temperatures. The decline in β with increasing drying temperature indicates an increase in the width of the relaxation spectrum. The order–disorder transformation zone of maize kernel was about 50–60 °C. Finally, TTS was successfully applied to predict the long-period relaxation modulus (up to 1600 h) and creep strain (up to 5000 h). These results show that maize kernel is a thermorheologically simple material. Further structural analyses (such as atomic force microscope and nuclear magnetic resonance analyses) are needed to clarify the molecular mechanism of the HVD kernels. The data acquired in this study can be used for maize processing and storage.

Author Contributions: Conceptualization, S.S. and A.S.; methodology, S.S. and J.X.; software, S.S.; validation, S.S.; formal analysis, S.S.; writing—original draft preparation, S.S.; writing—review and editing, A.S. and J.X.; visualization, A.S. and J.X.; project administration, S.S.; funding acquisition, S.S. All authors have read and agreed to the published version of the manuscript.

Data Availability Statement: Data are contained within the article.

Conflicts of Interest: The authors declare no conflict of interest.

References

1. Jiang, J.; Xing, F.; Wang, C.; Zeng, X.; Zou, Q. Investigation and development of maize fused network analysis with multi-omics. *Plant Physiol. Biochem.* **2019**, *141*, 380–387. [CrossRef] [PubMed]
2. Li, H.; Wang, Y.; Xue, J.; Xie, R.; Wang, K.; Zhao, R.; Liu, W.; Ming, B.; Hou, P.; Zhang, Z.; et al. Allocation of maize varieties according to temperature for use in mechanical kernel harvesting in Ningxia, China. *Int. J. Agric. Biol. Eng.* **2021**, *14*, 20–28. [CrossRef]
3. Bradford, K.J.; Dahal, P.; Van Asbrouck, J.; Kunusoth, K.; Bello, P.; Thompson, J.; Wu, F. The dry chain: Reducing postharvest losses and improving food safety in humid climates. *Trends Food Sci. Technol.* **2018**, *71*, 84–93. [CrossRef]
4. Bazyma, L.A.; Guskov, V.P.; Basteev, A.V.; Lyashenko, A.M.; Lyakhno, V.; Kutovoy, V.A. The investigation of low temperature vacuum drying processes of agricultural materials. *J. Food Eng.* **2006**, *74*, 410–415. [CrossRef]
5. Maskan, M. Microwave/air and microwave finish drying of banana. *J. Food Eng.* **2000**, *44*, 71–78. [CrossRef]
6. Arévalo-Pinedo, A.; Murr, F.E.X. Kinetics of vacuum drying of pumpkin (Cucurbita maxima): Modeling with shrinkage. *J. Food Eng.* **2006**, *76*, 562–567. [CrossRef]
7. Onwude, D.I.; Hashim, N.; Chen, G. Recent advances of novel thermal combined hot air drying of agricultural crops. *Trends Food Sci. Technol.* **2016**, *57*, 132–145. [CrossRef]
8. Essex, E. Objective measurements for texture in foods. *J. Texture Stud.* **1969**, *1*, 19–37. [CrossRef]
9. Waananen, K.M.; Okos, M.R. Stress-relaxation properties of yellow-dent corn kernels under uniaxial loading. *Trans. ASAE* **1992**, *35*, 1249–1258. [CrossRef]
10. Ravanbod, R.; Torkaman, G.; Esteki, A. Biotribological and biomechanical changes after experimental haemarthrosis in the rabbit knee. *Haemophilia* **2011**, *17*, 124–133. [CrossRef] [PubMed]
11. Wang, P.; Wang, L.; Li, D.; Huang, Z.; Adhikari, B.; Chen, X.D. The stress-relaxation behavior of rice as a function of time, moisture and temperature. *Int. J. Food Eng.* **2017**, *13*, 20160162. [CrossRef]
12. Li, Q.; Li, D.; Wang, L.; Özkan, N.; Mao, Z. Dynamic viscoelastic properties of sweet potato studied by dynamic mechanical analyzer. *Carbohyd. Polym.* **2010**, *79*, 520–525. [CrossRef]
13. Abedi, F.M.; Takhar, P.S. Stress relaxation properties of bananas during drying. *J. Texture Stud.* **2022**, *53*, 146–156. [CrossRef] [PubMed]

14. Ditudompo, S.; Takhar, P.S.; Ganjyal, G.M.; Hanna, M.A. The effect of temperature and moisture on the mechanical properties of extruded cornstarch. *J. Texture Stud.* **2013**, *44*, 225–237. [CrossRef]

15. Ozturk, O.K.; Takhar, P.S. Physical and viscoelastic properties of carrots during drying. *J. Texture Stud.* **2020**, *51*, 532–541. [CrossRef]

16. Shahgholi, G.; Latifi, M.; Jahanbakhshi, A. Potato creep analysis during storage using experimental measurement and finite element method (FEM). *J. Food Process Eng.* **2020**, *43*, e13522. [CrossRef]

17. Lin, C.; He, G.; Liu, J.; Pan, L.; Liu, S.; Li, J.; Guo, S. Construction and non-linear viscoelastic properties of nano-structure polymer bonded explosives filled with graphene. *Compos. Sci. Technol.* **2018**, *160*, 152–160. [CrossRef]

18. Ferry, J.D. *Viscoelastic Properties of Polymers*, 3rd ed.; John Wiley & Sons: New York, NY, USA, 1980; p. 273.

19. Xu, Y. Creep behavior of natural fiber reinforced polymer composites. Ph.D. Thesis, Louisiana State University, Baton Rouge, LA, USA, 2009.

20. Vaidyanathan, T.K.; Vaidyanathan, J. Validity of predictive models of stress relaxation in selected dental polymers. *Dent. Mater.* **2015**, *31*, 799–806. [CrossRef]

21. Kontogiorgos, V. Linear viscoelasticity of gluten: Decoupling of relaxation mechanisms. *J. Cereal Sci.* **2017**, *75*, 286–295. [CrossRef]

22. Koutsomichalis, A.; Kalampoukas, T.; Mouzakis, D.E. Mechanical testing and modeling of the time–temperature superposition response in hybrid fiber reinforced composites. *Polymers* **2021**, *13*, 1178. [CrossRef]

23. Amjadi, M.; Fatemi, A. Creep behavior and modeling of high-density polyethylene (HDPE). *Polym. Test.* **2021**, *94*, 107031. [CrossRef]

24. Ghosh, S.K.; Rajesh, P.; Srikavya, B.; Rathore, D.K.; Prusty, R.K.; Ray, B.C. Creep behaviour prediction of multi-layer graphene embedded glass fiber/epoxy composites using time-temperature superposition principle. *Compos. Part A Appl. Sci. Manuf.* **2018**, *107*, 507–518. [CrossRef]

25. Xue, C.; Gao, H.; Hu, Y.; Hu, G. Experimental test and curve fitting of creep recovery characteristics of modified graphene oxide natural rubber and its relationship with temperature. *Polym. Test.* **2020**, *87*, 106509. [CrossRef]

26. Sheng, S.; Wang, L.; Li, D.; Mao, Z.; Adhikari, B. Viscoelastic behavior of maize kernel studied by dynamic mechanical analyzer. *Carbohyd. Polym.* **2014**, *112*, 350–358. [CrossRef]

27. Wang, Z.D.; Zhao, X.X. Modeling and characterization of viscoelasticity of PI/SiO$_2$ nanocomposite films under constant and fatigue loading. *Mater. Sci. Eng. A* **2008**, *486*, 517–527. [CrossRef]

28. Tajvidi, M.; Falk, R.H.; Hermanson, J.C. Time–temperature superposition principle applied to a kenaf-fiber/high-density polyethylene composite. *J. Appl. Polym. Sci.* **2005**, *97*, 1995–2004. [CrossRef]

29. Xu, Y.; Wu, Q.; Lei, Y.; Yao, F. Creep behavior of bagasse fiber reinforced polymer composites. *Bioresour. Technol.* **2010**, *101*, 3280–3286. [CrossRef]

30. Jabbar, A.; Militký, J.; Madhukar Kale, B.; Rwawiire, S.; Nawab, Y.; Baheti, V. Modeling and analysis of the creep behavior of jute/green epoxy composites incorporated with chemically treated pulverized nano/micro jute fibers. *Ind. Crop. Prod.* **2016**, *84*, 230–240. [CrossRef]

31. Zhang, Y.; Sun, Z.; Li, Y.; Huang, P.; Chen, Q.; Fu, S. Tensile creep behavior of short-carbon-fiber reinforced polyetherimide composites. *Compos. Part B Eng.* **2021**, *212*, 108717. [CrossRef]

32. Rajan, S.; Sutton, M.A.; Wehbe, R.; Gurdal, Z.; Kidane, A.; Emri, I. Characterization of viscoelastic bending stiffness of uncured carbon-epoxy prepreg slit tape. *Compos. Struct.* **2021**, *275*, 114295. [CrossRef]

33. Liu, Y.; Wang, Y.; Lv, W.; Li, D.; Wang, L. Freeze-thaw and ultrasound pretreatment before microwave combined drying affects drying kinetics, cell structure and quality parameters of Platycodon grandiflorum. *Ind. Crop. Prod.* **2021**, *164*, 113391. [CrossRef]

34. Qiao, J.; Wu, Y.; Li, L. Effect of filler content on the stress relaxation behavior of fly ash/polyurea composites. *Polym. Test.* **2020**, *81*, 106168. [CrossRef]

35. Zhao, N.; Li, B.; Zhu, Y.; Li, D.; Wang, L. Viscoelastic analysis of oat grain within linear viscoelastic region by using dynamic mechanical analyzer. *Int. J. Food Eng.* **2020**, *16*, 20180350. [CrossRef]

36. Ozturk, O.K.; Takhar, P.S. Stress relaxation behavior of oat flakes. *J. Cereal Sci.* **2017**, *77*, 84–89. [CrossRef]

37. Sozer, N.; Dalgic, A.C. Modelling of rheological characteristics of various spaghetti types. *Eur. Food Res. Technol.* **2007**, *225*, 183–190. [CrossRef]

38. Khan, M.; Nagy, S.A.; Karim, M.A. Transport of cellular water during drying: An understanding of cell rupturing mechanism in apple tissue. *Food Res. Int.* **2018**, *105*, 772–781. [CrossRef]

39. Wang, J.; Mujumdar, A.S.; Deng, L.Z.; Gao, Z.J.; Xiao, H.W.; Raghavan, G. High-humidity hot air impingement blanching alters texture, cell-wall polysaccharides, water status and distribution of seedless grape. *Carbohydr. Polym* **2018**, *194*, 9–17. [CrossRef]

40. Ozturk, O.K.; Singh Takhar, P. Selected physical and viscoelastic properties of strawberries as a function of heated-air drying conditions. *Dry. Technol.* **2019**, *37*, 1833–1843. [CrossRef]

41. Sandhu, J.S.; Takhar, P.S. Effect of frying parameters on mechanical properties and microstructure of potato disks. *J. Texture Stud.* **2015**, *46*, 385–397. [CrossRef]

42. Zhu, Y.; Fu, N.; Li, D.; Wang, L.; Chen, X.D. Physical and viscoelastic properties of different moisture content highland barley kernels. *Int. J. Food Eng.* **2017**, *13*, 20170186. [CrossRef]

43. Ornaghi, H.L.; Monticeli, F.M.; Neves, R.M.; Zattera, A.J.; Cioffi, M.O.H.; Voorwald, H.J.C. Effect of stacking sequence and porosity on creep behavior of glass/epoxy and carbon/epoxy hybrid laminate composites. *Compos. Commun.* **2020**, *19*, 210–219. [CrossRef]

44. Hao, A.; Chen, Y.; Chen, J.Y. Creep and recovery behavior of kenaf/polypropylene nonwoven composites. *J. Appl. Polym. Sci.* **2014**, *131*, 8864–8874. [CrossRef]

45. Militký, J.; Jabbar, A. Comparative evaluation of fiber treatments on the creep behavior of jute/green epoxy composites. *Compos. Part B Eng.* **2015**, *80*, 361–368. [CrossRef]

46. Ahmed, J. Optimization of high-pressure-assisted xanthan gum dispersions for the maximization of rheological moduli: Application of time-pressure/ temperature superposition principle. *Food Hydrocolloid.* **2022**, *122*, 107080. [CrossRef]

47. Mateyawa, S.; Xie, D.F.; Truss, R.W.; Halley, P.J.; Nicholson, T.M.; Shamshina, J.L.; Rogers, R.D.; Boehm, M.W.; Mcnally, T. Effect of the ionic liquid 1-ethyl-3-methylimidazolium acetate on the phase transition of starch: Dissolution or gelatinization? *Carbohyd. Polym.* **2013**, *94*, 520–530. [CrossRef] [PubMed]

48. Kontogiorgos, V.; Shah, P.; Bills, P. Influence of supramolecular forces on the linear viscoelasticity of gluten. *Rheol. Acta* **2016**, *55*, 187–195. [CrossRef]

49. Ahmed, J. Effect of pressure, concentration and temperature on the oscillatory rheology of guar gum dispersions: Response surface methodology approach. *Food Hydrocolloid.* **2021**, *113*, 106554. [CrossRef]

50. Nakada, M.; Miyano, Y.; Cai, H.; Kasamori, M. Prediction of long-term viscoelastic behavior of amorphous resin based on the time-temperature superposition principle. *Mech. Time Depend. Mat.* **2011**, *15*, 309–316. [CrossRef]

51. Yusoff, N.I.M.; Jakarni, F.M.; Nguyen, V.H.; Hainin, M.R.; Airey, G.D. Modelling the rheological properties of bituminous binders using mathematical equations. *Constr. Build. Mater.* **2013**, *40*, 174–188. [CrossRef]

52. Singh, A.P.; Lakes, R.S.; Gunasekaran, S. Viscoelastic characterization of selected foods over an extended frequency range. *Rheol. Acta* **2006**, *46*, 131–142. [CrossRef]

53. Sun, S.; Song, Y.; Zheng, Q. Morphology and mechanical properties of thermo-molded bioplastics based on glycerol-plasticized wheat gliadins. *J. Cereal Sci.* **2008**, *48*, 613–618. [CrossRef]

54. Ahmed, J. Applicability of time–temperature superposition principle: Dynamic rheology of mung bean starch blended with sodium chloride and sucrose—Part 2. *J. Food Eng.* **2012**, *109*, 329–335. [CrossRef]

55. Herum, F.L.; Mensah, J.K.; Barre, H.J.; Majidzadeh, K. Viscoelastic behavior of soybeans due to temperature and moisture content. *Trans. ASAE* **1979**, *22*, 1219–1224. [CrossRef]

56. Meza, B.E.; Verdini, R.A.; Rubiolo, A.C. Temperature dependency of linear viscoelastic properties of a commercial low-fat soft cheese after frozen storage. *J. Food Eng.* **2012**, *109*, 475–481. [CrossRef]

57. Altay, F.; Gunasekaran, S. Rheological evaluation of gelatin–xanthan gum system with high levels of co-solutes in the rubber-to-glass transition region. *Food Hydrocolloid.* **2012**, *28*, 141–150. [CrossRef]

58. Contreras Mateus, M.D.; López López, M.T.; Ariza-León, E.; Chaves Guerrero, A. Rheological implications of the inclusion of ferrofluids and the presence of uniform magnetic field on heavy and extra-heavy crude oils. *Fuel* **2021**, *285*, 119184. [CrossRef]

59. Yildiz, M.E.; Kokini, J.L. Determination of Williams–Landel–Ferry constants for a food polymer system: Effect of water activity and moisture content. *J. Rheol.* **2001**, *45*, 903–912. [CrossRef]

60. Altay, F.; Gunasekaran, S. Mechanical spectra and calorimetric evaluation of gelatin–xanthan gum systems with high levels of co-solutes in the glassy state. *Food Hydrocolloid.* **2013**, *30*, 531–540. [CrossRef]

61. Peleg, M. On the use of the WLF model in polymers and foods. *Crit. Rev. Food Sci.* **1992**, *32*, 59–66. [CrossRef]

62. Li, M.; Li, D.; Wang, L.; Adhikari, B. Creep behavior of starch-based nanocomposite films with cellulose nanofibrils. *Carbohyd. Polym.* **2015**, *117*, 957–963. [CrossRef]

63. Shi, A.; Wang, L.; Li, D.; Adhikari, B. Characterization of starch films containing starch nanoparticles. Part 2: Viscoelasticity and creep properties. *Carbohyd. Polym.* **2013**, *96*, 602–610. [CrossRef]

64. Laplante, G.; Lee-Sullivan, P. Moisture effects on FM300 structural film adhesive: Stress relaxation, fracture toughness, and dynamic mechanical analysis. *J. Appl. Polym. Sci.* **2005**, *95*, 1285–1294. [CrossRef]

65. Ngai, K.L.; Rajagopal, A.K.; Teitler, S. Slowing down of relaxation in a complex system by constraint dynamics. *J. Chem. Phys.* **1988**, *88*, 5086–5094. [CrossRef]

66. Enrione, J.I.; Sáez, C.; López, D.; Skurtys, O.; Acevedo, C.; Osorio, F.; Macnaughtan, W.; Hill, S. Structural relaxation of salmon gelatin films in the glassy state. *Food Bioprocess Technol.* **2012**, *5*, 2446–2453. [CrossRef]